Advances in Water Resources 132 (2019) 103386

Contents lists available at ScienceDirect

Advances in Water Resources

journal homepage: www.elsevier.com/locate/advwatres

Short communication

Aging and mixing as pseudo-chemical-reactions between, and on, particles: Perspectives on particle interaction and multi-modal ages in hillslopes and streams

David A. Benson[a,*], Michael J. Schmidt[a], Diogo Bolster[b], Ciaran Harman[c], Nicholas B. Engdahl[d]

[a] Hydrologic Science and Engineering, Colorado School of Mines, Golden, CO 80401, USA
[b] Department of Civil and Environmental Engineering and Earth Sciences, University of Notre Dame, Notre Dame, IN 46556, USA
[c] Johns Hopkins University, USA
[d] Department of Civil and Environmental Engineering, Washington State University, Pullman, WA, 99164, USA

ARTICLE INFO

Keywords:
Particle methods
Mixing
Aging
Age distribution

ABSTRACT

The particle-tracking method was recently extended to allow inter-particle mass transfer and arbitrarily complex reactions by allowing each particle to represent any number of distinct chemical compounds. This methodology allows the tracking (and broadening due to mixing) of the age probability density function (PDF) on each particle. Aquifer heterogeneity leads to channeling and multi-modal age PDFs in stream samples. This observation supports the concept of age classes but clearly shows the more complicated interplay of dispersion, mixing, and travel times on the age distributions.

1. Introduction

Direct simulation of age in hydrologic systems is often necessary when interpreting environmental tracers, assessing water quality, and evaluating contamination risks, among other possible needs. Both Eulerian and Lagrangian methods have been used for these purposes in the past and each method has tradeoffs. Eulerian simulations (Goode, 1996; Varni and Carrera, 1998; Cornaton and Perrochet, 2006) can simulate the moments of the age distribution, or the full distribution, in each cell of the model but these are computationally expensive, generate overly diffuse probability density functions (PDFs) because of the numerical dispersion inherent in heterogeneous velocity fields, and are difficult to generalize to transient fields (Cornaton, 2012). Classical Lagrangian particle tracking eliminates the numerical dispersion by design (Labolle et al., 1996) and reduces the computational load because each particle in a classical particle tracking (PT) scheme is independent from the others. However, the PT approach comes with the implicit assumption that mixing of particle ages does not occur until a sampling is taken (i.e., at monitoring wells), at which point the ages of each particle in the sample create a PDF. This can lead to step-wise or abruptly varying PDFs (Weissmann et al., 2002; Engdahl et al., 2016), which are not expected in natural systems. Conceptually this is identical to streamline/streamtube models but the lack of mixing in these models can significantly impact their results (Herrera et al., 2010; Cirpka et al., 2015; Sanz-Prat et al., 2015). Put simply, Eulerian techniques overestimate age mixing while classical PT techniques underestimate mixing. A compromise between these end members would more closely represent reality (i.e., limiting numerical dispersion while still allowing evolution of age PDFs as waters from different sources mix) but this is a deficiency in the capabilities of the currently available methods for simulating age.

The classical PT method is limited to a Dirac-delta distribution for the age of each particle, but simulating age mixing requires storing a representative age PDF on each particle and also a dynamic and realistic particle/particle interaction model. A recent series of advances provides the algorithms needed to explicitly model Lagrangian age-mixing, but has yet to be applied to this task. The first component allowed particle interactions via birth/death chemical reaction processes, where the likelihood of reacting was found to be a function of the dispersion coefficients of the particles and their separation distances, combined to form their co-location probabilities (Benson and Meerschaert, 2008). This was later generalized (Bolster et al., 2016) so that the birth/death process was replaced by a change to each particle's mass, keeping the size of the particle ensemble constant over time. The last necessary algorithm (Benson and Bolster, 2016) allows any number of chemical species and reactions on particles: each particle is treated as a moving container that carries an arbitrary number of chemical components; the masses of each component are exchanged between different particles to represent mixing. The degree of mixing remains a function of the particle/particle co-location probability. Conservative quantities can be represented this

* Corresponding author.
E-mail address: dbenson@mines.edu (D.A. Benson).

https://doi.org/10.1016/j.advwatres.2019.103386
Received 9 May 2019; Received in revised form 19 July 2019; Accepted 1 August 2019
Available online 2 August 2019

way, so that the algorithm can be extended to represent dynamic water age-mixing between particles.

This technical note proposes a modification of the recent reactive PT methods where chemical components are replaced with the bins of a discrete age PDF, and aging is represented as a pseudo-reaction. Each particle is initialized as a Dirac-delta distribution when it enters the domain and functions as a "clock" where all of its age-mass increases by one time unit every time step; importantly, this satisfies the requirement that there can be no artificial dispersion in the age dimension (Ginn, 1999; Engdahl et al., 2012). However, diffusive mixing between particles allows each PDF to evolve away from its initial Dirac-delta into an arbitrary, non-parametric PDF as long as the number of bins is sufficient enough to hold all the ages. Since the aging velocity is always the same as the time step, a unit Courant number is achieved along the age dimension, thus the proposed scheme achieves the goal of eliminating numerical dispersion while allowing age mixing between streamlines. The approach is demonstrated on an idealized hillslope domain with distributed recharge under homogeneous and heterogeneous hydraulic conductivity (K) fields. The latter fields generate multi-modal age distributions that are not discernible using the classic PT method.

2. Review of inter-particle mixing

Denote by m_i^A the mass of species A on particle i. For a bimolecular reaction $A + B \rightarrow C$, with rate expression $d[A]/dt = d[B]/dt = -k[A][B]$, and using a (well-mixed) thermodynamic rate coefficient k, a first-order expression of mass change over time step Δt is Bolster et al. (2016):

$$\Delta m_i^A = \sum_{j \neq i} m_j^B m^A (k\Delta t) v_{ij}, \tag{1}$$

where v_{ij} is the probability density function (PDF) of co-location of the i^{th} and j^{th} particle over the timestep (Benson and Meerschaert, 2008). This probability depends on the perceived physics of random motion, but for Brownian motion this is a simple convolution of the individual (Gaussian) location densities in d-dimensions. If the i^{th} and j^{th} particles (located at vectors x_i and x_j) have local isotropic dispersion coefficients D_i and D_j, then

$$v_{ij} = \left(4\pi(D_i + D_j)\Delta t\right)^{-d/2} \exp\left[-||x_i - x_j||^2 / \left(4(D_i + D_j)\Delta t\right)\right], \tag{2}$$

i.e., a Gaussian with a variance that is the sum of the two location density variances.

The mixing of the same species between particles may be viewed as a "bimolecular" reaction of the form $pA + qA \rightarrow \frac{p+q}{2}A + \frac{p+q}{2}A$. This reaction also happens with the probability described above, so that the mixing process on the i^{th} particle can be written (Benson and Bolster, 2016):

$$\Delta m_i^A = \sum_j \frac{1}{2}\left(m_j^A - m_i^A\right) P_{ij}, \tag{3}$$

where the total probability $P_{ij} \propto v_{ij}$ is normalized so that $\sum_j P_{ij} = 1$. A pseudo-code that shows how the model works and a snippet of matlab code that performs inter-particle mixing is shown in Fig. 1. While this double-looping code is neither the fastest nor most accurate method (Schmidt et al., 2018; Engdahl et al., 2019), we include it here to demonstrate the simplicity of the algorithm. In practice, the mass transfer is best performed in a single matrix operation that provides a physical basis for more arbitrary smoothed-particle-hydrodynamics (SPH) methods (Sole-Mari et al., 2019).

3. Aging

Particles may be given a set of species that represent ages from 0 to a maximum of the total simulation time t. Define an age discretization $k = 0, 1, \ldots, K$ and denote these species ρ_k, with age $k\Delta a$. Without loss of generality we use equal age and timestep sizes $\Delta a = \Delta t$. The mixing at each time step follows (3). The aging "reaction" $\rho_k \rightarrow \rho_{k+1}$ simply moves all water mass from each bin k to bin $k + 1$ (see also Massoudieh et al., 2017; Engdahl et al., 2012). Any new particles introduced to the domain have a certain mass given by the specifics of the problem and all mass in those particles is placed in bin $k = 0$. Any particles removed from the domain cease aging. Here we use unit initial mass for ρ_0, and conservation of mass implies that $\rho_k \approx \rho(a, t)$ is a numerical approximation of the continuous PDF of age a at a given time t. Clearly, if no mixing between particles takes place, the simulated mass PDF on each particle remains a Dirac-delta function of the particle's elapsed time in the system, as has been done in prior PT simulations (e.g., Weissmann et al., 2002). However, if mixing between particles takes place, then water of different ages will, with some probability, move around the domain between particles in exact accordance with the specified local physics of mixing.

4. Numerical implementation considerations

One of the advantages of the classical particle-tracking algorithm is that the Courant-number stability requirement inherent in Eulerian (grid-based) codes is lifted. The particles may be moved for different timesteps Δt with no instability. Because of the potentially large discrepancy of particle velocities, immense computational gains may be had by allowing slower particles to move for longer times between recalculating local velocity or dispersion coefficients. However, this invites two complications in the present model. First, the aging algorithm given above assumes that the timestep size and the age bins are equal and the same for all particles. Then the hyperbolic (wave) equation $\frac{\partial \rho}{\partial t} = -\frac{\partial \rho}{\partial a}$ is solved exactly, with no numerical age dispersion, using first differences and setting $\Delta a = \Delta t$. Various higher-order techniques may be used if $\Delta t \leq \Delta a$ on any particle (see the review of second-order techniques in the appendix of Benson et al. (2017)). This equation does carry a Courant-number type restriction that $\Delta t \leq \Delta a$, so that the discretization of the age PDF should be done with care if variable timesteps are used. Second, choosing the same timestep for all particles allows (2) to be implemented as-is for the inter-particle mixing. But recognizing that (2) is simply the convolution of the i^{th} and j^{th} particle location densities lets us expand somewhat to

$$v_{ij} = \left(4\pi\left(D_i\Delta t_i + D_j\Delta t_j\right)\right)^{-d/2} \exp\left[-||x_i - x_j||^2 / \left(4\left(D_i\Delta t_i + D_j\Delta t_j\right)\right)\right], \tag{4}$$

which allows each particle to use its unique optimal timestep Δt_i. Ideally, one would choose to classify the particles into integer "classes" of mixing calculation frequency. The fastest class of particles are calculated every timestep, the second class would be calculated every other timestep, etc. Because the timesteps are not all equal, an occasional short timestep is implemented to "sync" all particles to the same elapsed time. While we did not choose variable timesteps in the examples that follow, we have implemented such an algorithm as proof-of-concept. The mixing algorithm itself, and therefore the entire model, is accurate to $\mathcal{O}(\Delta t)$, so enlarging the timesteps of some particles may engender errors that are transferred between particles. There are also several technical details that are outside the scope of this study. A detailed analysis of the magnitude of computational gains and increase in errors among the advection, dispersion, mixing, and aging algorithms is the subject of a future manuscript.

It is also difficult to directly compare the accuracy and computational demands of Lagrangian versus Eulerian methods. Adding the many age bins has an equal effect on both in terms of added memory and calculations. In heterogeneous velocity fields, the Eulerian methods suffer significantly from numerical dispersion and therefore typically require much finer spatial discretization (i.e., more nodes than particles, see Benson et al. (2017)). For high Peclet number flows, the grid-Peclet number requirement in Eulerian methods can be much more restrictive than any Courant-number restrictions shared by both. In some cases, a super-computer may be required for Eulerian simulation of mixing-limited reaction (Benson et al., 2019a), while the same problem using the newer Lagrangian methods can be run in minutes on a laptop PC.

pseudo-code

```
Specify constants including # of age pdf bins (Nage) and # of particles (Npart);

Create a matrix X with Npart rows; Columns 1 to 3 have x, y, z particle positions; columns
6 through Nage + 5 are age pdf values (columns 4 and 5 for future use);

Begin time loop;
      Add new particles, move all particles according to local physics;
% comment ----- Perform mixing between all particles:
      For each particle, find all nearby particles within 3 diffusion distances using KDTREE;
      Loop through all particles i = 1 to Npart
            For particles near and including i,
                  Sum collision probabilites;
                  Normalize probabilities so sum = 1;
            end for
            For nearby particles with indexes j >= i
                  Transfer mass between i and j in every age bin weighted by collision prob;
            End for loop for nearby particles
      End loop for all i particles
% comment - done with mixing between all particles
      Sample particles that leave domain and create average age pdf from ensemble;
      Simulation finished?;
End time loop
```

MATLAB code for mixing portion

```
% X has columns 1:3 for particle x,y,z position, and 6:Nage+5 for age bins.
% There are Ntot rows for the Ntot particles. D is scalar. Use kd-tree search.

  dist=3*sqrt(2*(2*D*dt)); % Look for nearby particles in radius=dist
  [idx r]=rangesearch(X(:,1:3),X(:,1:3),dist,'SortIndices',false);

 for i=1:Ntot
   jparts=idx{i};   % This is the indices list of nearby particles to i
   s=r{i};          % Associated distances
   Ptot=(1/(8*pi*D*dt)).*exp(s.^2./(-8*D*dt)); % 2-d co-location PDFs
   rescale=sum(Ptot);  % Rescale constant for total probability
   Ptot=Ptot/rescale;
   s=s(jparts>i);        % Only mass transfer once (don't do j-->i AND i-->j)
   Ptot=Ptot(jparts>i);
   apple=jparts(jparts>i);
   if(~isempty(apple)) % Only if there are nearby particles to i
       for j=1:length(apple)
          jnow=apple(j);    % Index of the current "other" particle
          dm = 0.5*(X(i,6:Nage+5)-X(jnow,6:Nage+5))*Ptot(j);
          %update particle ages in both particles
          X(i,6:Nage+5)=max(0,(X(i,6:Nage+5)-dm));
          X(jnow,6:Nage+5)=max(0,(X(jnow,6:Nage+5)+dm));
       end
   end   % end if-loop for more than one particle
 end     % end for-loop for each (ith) particle
```

Fig. 1. Top: Pseudo-code for particle tracking and age-mixing code. Bottom: Explicit looping-over-particles Matlab code for the inter-particle mixing portion of the algorithm.

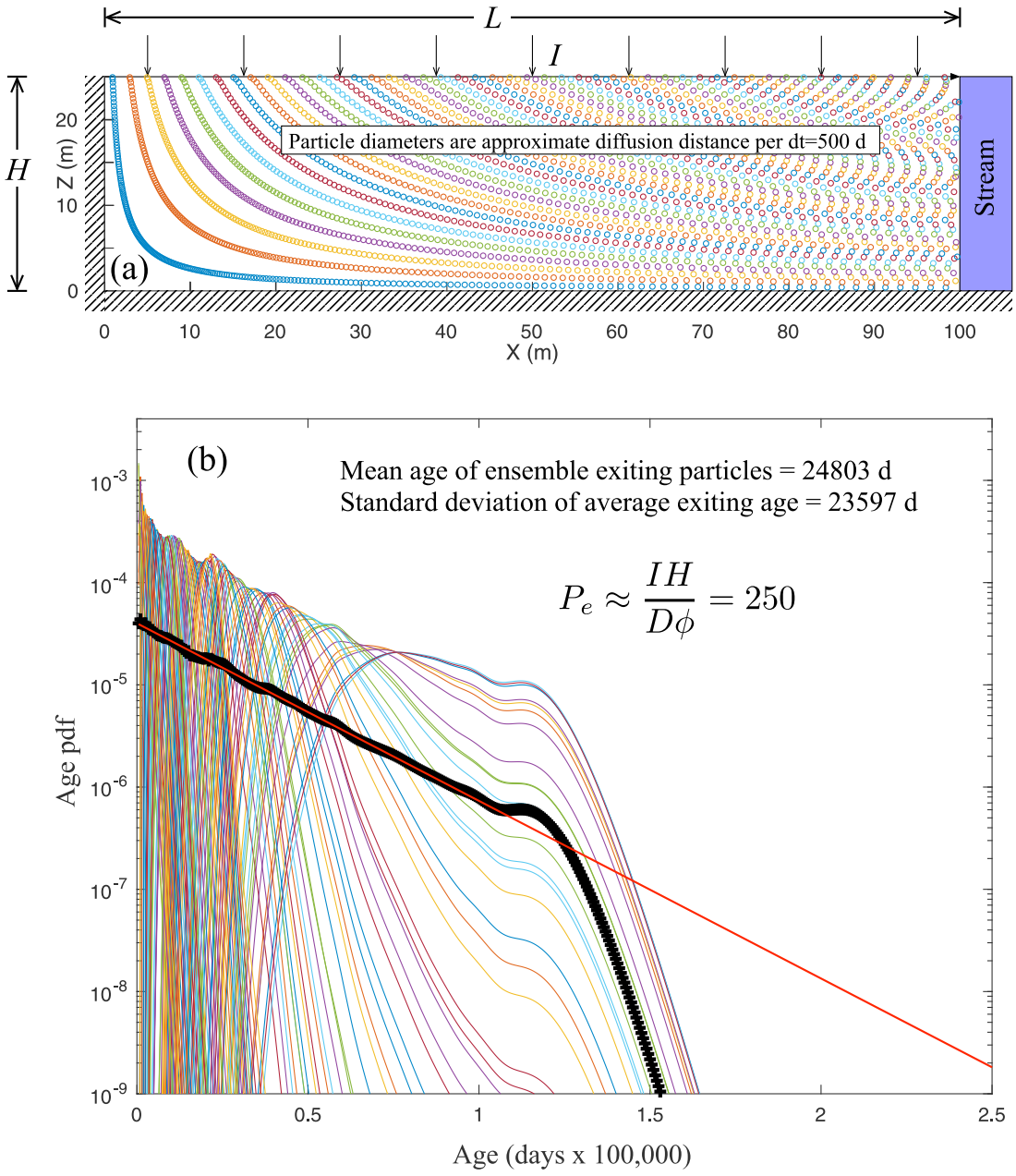

Fig. 2. a) Schematic and particle positions at t=250,000 d. Only every other particle trace is shown for clarity. Circle diameters denote approximate diffusion distance $2\sqrt{2D\Delta t}$ over $\Delta t = 500$ d. b) Age PDFs of all exiting particles (colored lines) and average age PDF (black "+" symbols). Analytic PDF for pure advection shown by red line. This simulation has Peclet number $P_e = \frac{IH}{D\phi} = 250$ and expected travel time = $H\phi/I = 25,000$ d. (For interpretation of the references to colour in this figure legend, the reader is referred to the web version of this article.)

5. Examples

To illustrate the functioning of the model, we use a very simple conceptualization of water transport in a perfectly rectangular "hillslope" aquifer that has uniform recharge from above and discharges to a completely penetrating stream on the right (Fig. 2a). The aquifer is given a width of $x = [0, L]$ m, a height of $z = [0, H]$ m, and a uniform porosity of $\phi = 0.25$. Because the water table is conceptualized as flat, the divergence-free condition for an incompressible fluid gives each streamline an analytic solution for velocity $v_x = ILx/(H\phi)$, $v_z = -Iz/\phi$, where we set $I = 2.5 \times 10^{-4}$ m/d as the vertical recharge into the aquifer. For these simulations, $L = 100$ m, $H = 25$ m. Particles are advected by this velocity field by forward Euler methods. The infiltration in each timestep is split among 100 evenly-spaced particles along the top boundary. Diffusive mass transfer is by (3) alone, i.e., no random walks are used to disperse particles (Schmidt et al., 2018). The simulations were run for 250,000 d (684 yr) with timesteps of 500 d, giving 500 age bins on each particle. Two simulations were run with spatially uniform dispersion, one with local dispersion coefficient set to approximately that of molecular diffusion ($D = 10^{-4}$ m^2/d) (Fig. 2) and another with a larger $D = 2.5 \times 10^{-3}$ m^2/d (Fig. 3). These values give approximate aquifer-average Peclet numbers of 250 and 10, respectively (see Appendix for derivation of the Peclet number).

Each simulation gives about the same calculated stream sample mean age (24,803 and 24,786 days (67.9 years) for lower and higher D, respectively). Because the average PDFs are reasonably close to an exponential

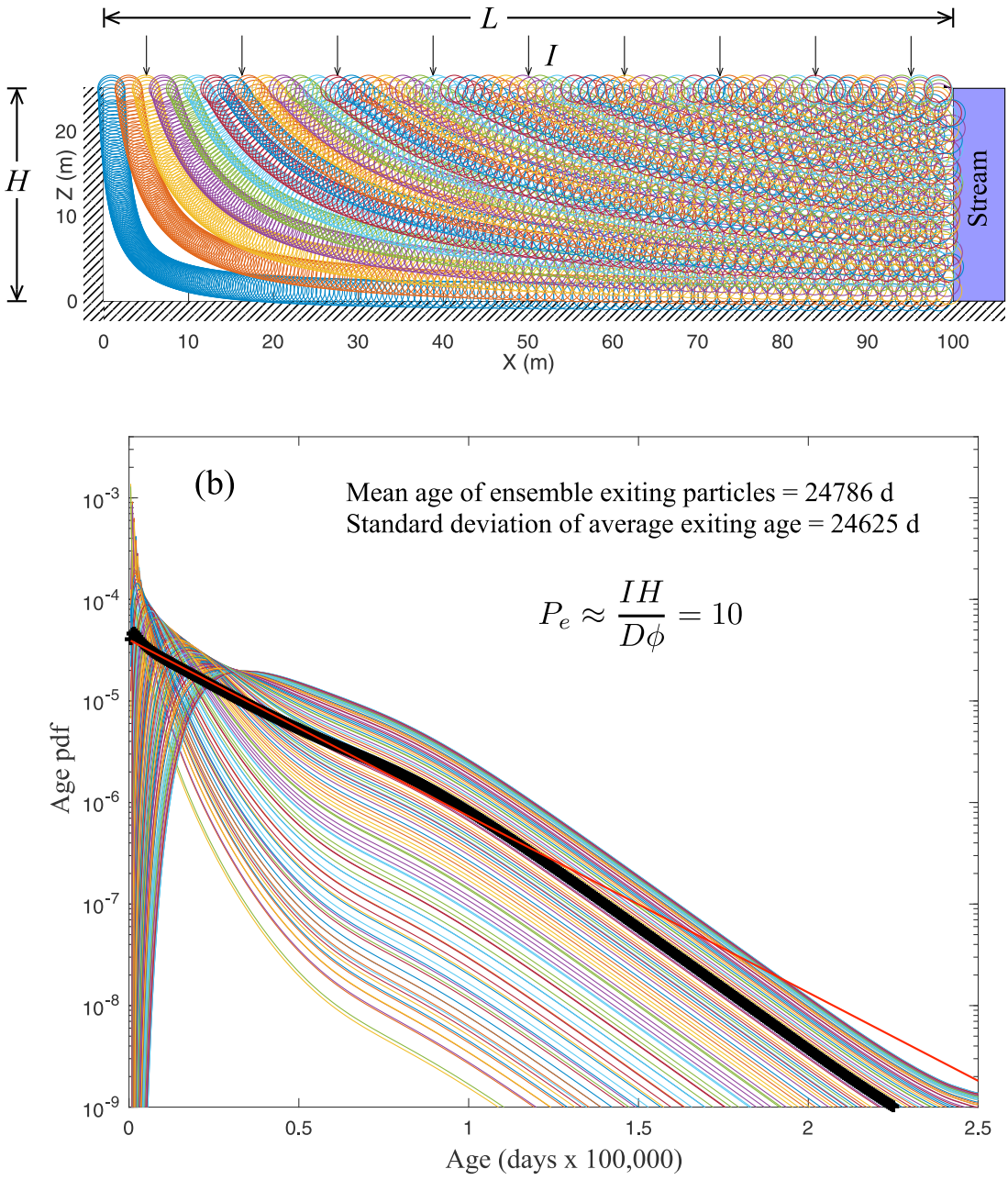

Fig. 3. a) Schematic and particle positions at t=250,000 d. Only every other particle trace is plotted for clarity. Circle diameters denote approximate diffusion distance $2\sqrt{2D\Delta t}$ over $\Delta t = 500$ d. b) Age PDFs of all exiting particles (colored lines) and average age PDF (black "+" symbols). Analytic PDF for pure advection shown by red line. This simulation has Peclet number $P_e = \frac{IH}{D\phi} = 10$ and expected travel time = $H/I = 25,000$ d. (For interpretation of the references to colour in this figure legend, the reader is referred to the web version of this article.)

function over the majority of age (which agrees with the pure advection case, see the Appendix), the standard deviations are also close to the means (23,597 and 24,625 days, respectively). These statistics are calculated by averaging the PDFs for all particles exiting the system in a single timestep after the system has equilibrated (heavy black "plus" symbols in Figs. 3b and 2b). For the lower dispersion coefficient, the age PDF for each particle is narrower, as is average "stream sample" PDF. However, in this simple system the average PDF is primarily based on the peak, or mean age, of each particle. In the case of higher D, even the fastest moving particles exchange significant older water among nearby particles. It is highly likely that many factors that influence segregation of waters will change this mixing dynamic. Here we only look at the combined effect of two: velocity-dependent dispersion and heterogeneous hydraulic conductivity (K), both of which should lead to "channeling" of flow and poorer mixing of slower-moving, older water (especially with higher K variability).

Here we chose an isotropic, velocity-dependent dispersion coefficient $D = \alpha|v|$, with an approximate Peclet number of 250 (see Appendix), which gives an isotropic dispersivity of $\alpha = 0.1$ m. First we used finite-differences to solve the steady velocity field within a heterogeneous K field with anisotropic, exponential correlation function (Fig. 4a). The K correlation lengths in the horizontal and vertical directions are 9 and 3 m, and the standard deviation of the natural logarithm of K was set to unity. The heterogeneous field gives rise to focusing of flow into preferential flow paths (Fig. 4b) that are discernible at steady state (Fig. 4c). The high-speed channels lead to well-mixed and

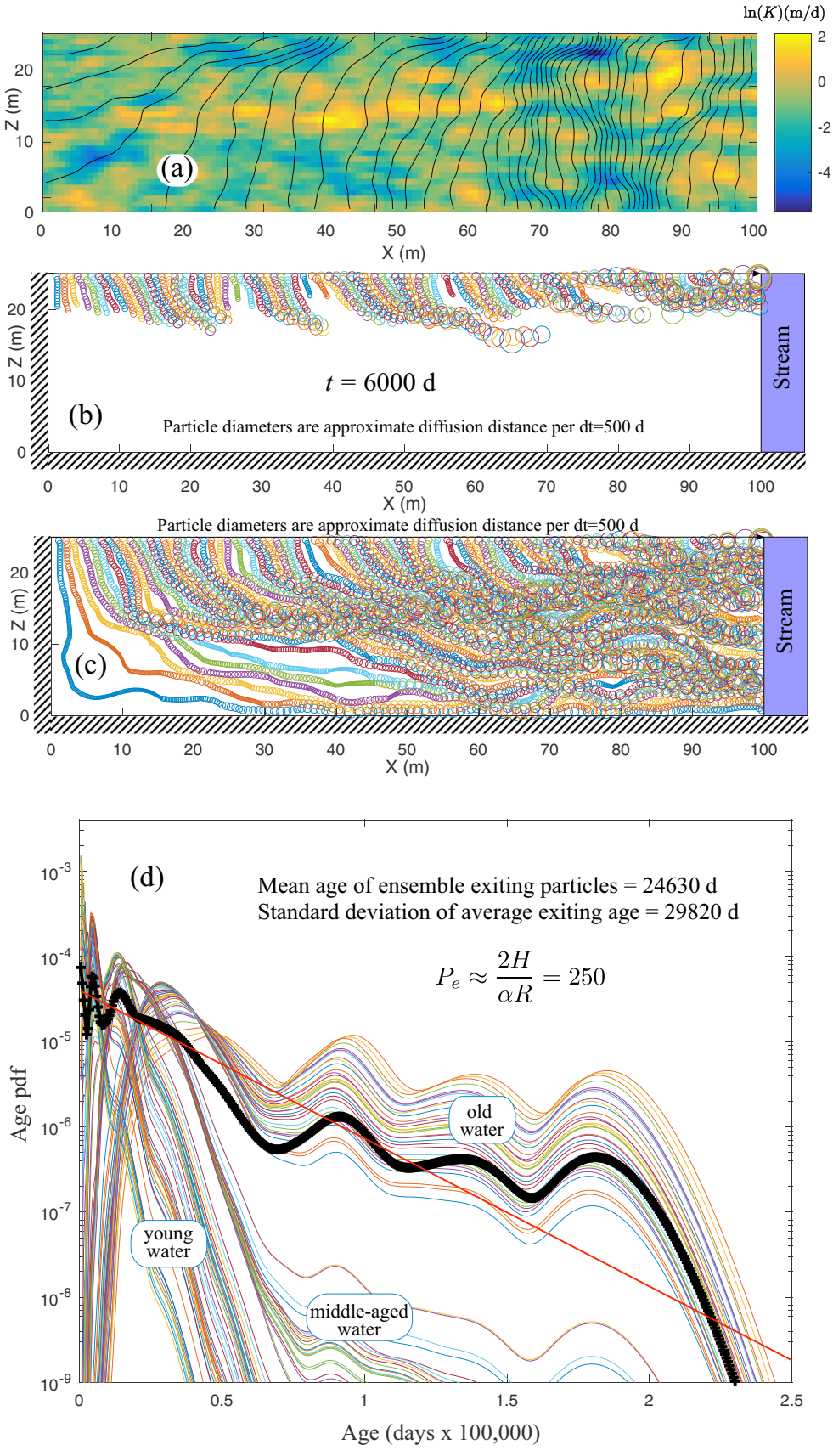

Fig. 4. a) Heterogeneous K distribution and head equipotentials (black curves) in same size aquifer as in Figs. 1 and 2; b) Particle positions at t=6,000 d. Circle diameters denote approximate diffusion distance $2\sqrt{2\alpha|v|\Delta t}$ over $\Delta t = 500$ d; c) Steady-state particle positions and dispersion distances; d) PDFs of all exiting particles (colored lines) and average age PDF (black "+" symbols). Analytic PDF for pure advection in homogeneous K shown by red line for comparison. This simulation has Peclet number $P_e \approx \frac{2H}{\alpha R} = 250$. (For interpretation of the references to colour in this figure legend, the reader is referred to the web version of this article.)

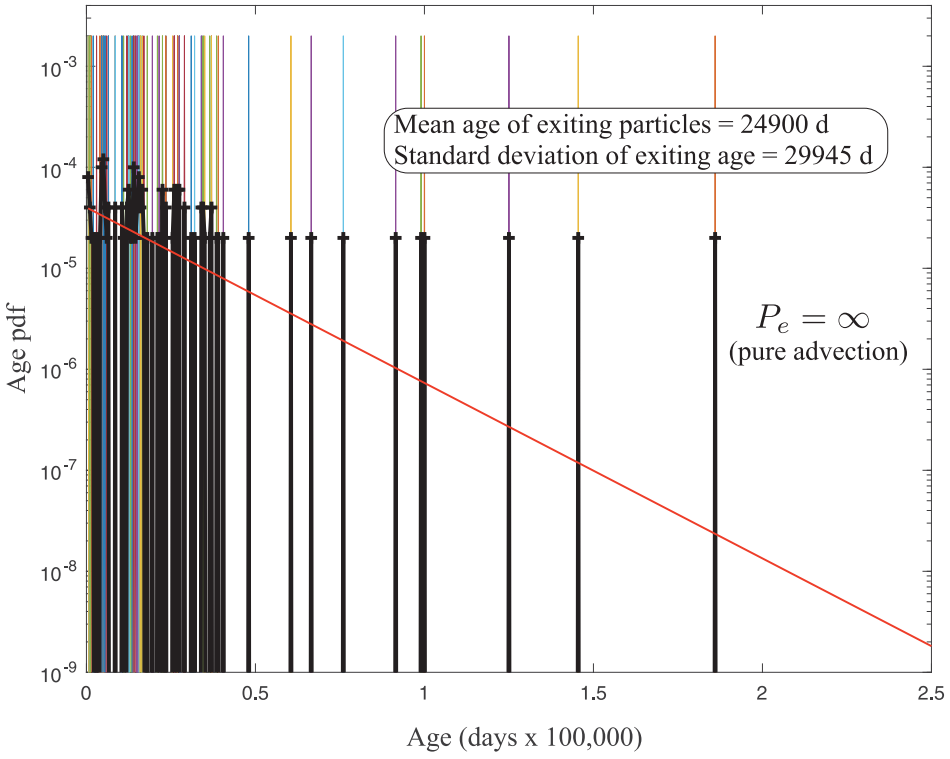

Fig. 5. Dirac-delta "PDFs" of all exiting particles (colored lines) and 100-particle average age PDF (black lines and "+" symbols) for pure advection ($P_e = \infty$). This simulation uses the same velocity distribution as Fig. 4. Numerical delta functions (colored lines) are Δt wide and $1/\Delta t$ tall.

distinct-age modes that enter the stream, but also leaves distinct poorly-mixed slow paths (e.g., see very bottom of Fig. 4c). Inspection of the PDFs of particles entering the stream reveals a multi-modal travel time PDF with clear "groups" of younger versus older water that correspond to the modes of the average PDF (Fig. 4d). Furthermore, the standard deviation of travel time has increased by 20% over the homogeneous case with the same aquifer-wide Peclet number.

We may compare the PDFs that arise during inter-particle mixing to those that must be inferred when using the previous method of non-interacting (Dirac-delta function) particles (Fig. 5). In this case, the delta-particles give similar estimates of mean and standard deviation of age, but it is nearly impossible to discern the several distinct age modes that are found in the interacting-particle case (Fig. 4d). Here a relatively large number of particles (100) are used to represent a stream "sample" and the creation of the average age PDF. In order to discern any structure in the real PDF, one would have to arbitrarily choose an interpolation kernel that almost certainly lacks the details of the mixing processes that are unique to each particle. In other words, due to particle/particle dependence, the shape of each particle age PDF (i.e., the kernel function needed post-process each Dirac delta particle) is too complex to capture by intuition (see also Benson et al. (2019b)).

We expect that other parameters that influence this mixing, such as aquifer aspect ratio and heterogeneity, anisotropic dispersion, K heterogeneity statistics, partitioning to immobile water phase(s), and spatio-temporal variability of recharge (for recent examples, see Massoudieh et al., 2017; Engdahl et al., 2012; Green et al., 2018; Koh et al., 2018), will significantly change the PDFs and will be explored in a future paper.

6. Conclusion

The particle mixing method for chemical reactions can simulate age distributions upon particles. These ages must mix between particles, which represent parcels of water; therefore, the PDF of age must be tracked on each particle in order to accurately simulate the age distribution of aquifer and stream water. When spatial heterogeneity of K and/or D is present, the age distribution becomes multi-modal, which is difficult or impossible to discern solely from particle transit times (i.e., Dirac-delta particle age PDFs).

Acknowledgments

This material is based upon work supported by, or in part by, the US Army Research Office under Contract/Grant number W911NF-18-1-0338. The authors were also supported by the National Science Foundation under awards EAR-1417145, DMS-1211667, DMS-1614586, EAR-1351625, EAR-1417264, EAR-1446236, CBET-1705770, and DMS-1911145, and the U.S. Department of Energy under award DE-SC0019123. All codes used to perform the simulations herein were written in matlab and are freely available from the corresponding author.

Appendix. Analytic Age Distributions for Pure Advection

For a constant infiltration (recharge) rate I evenly distributed across a rectangular hillslope of length L and height H (Fig. 2a), the Darcy discharge exiting the right hand side is IL/H for incompressible steady flow, so that the linear increase in x-direction velocity follows $dx/dt = v_x(x) = \frac{Ix}{H\phi}$. (The divergence-free condition $\frac{\partial v_x}{\partial x} = -\frac{\partial v_z}{\partial z}$ gives $v_z(z) = \frac{-Iz}{H\phi}$.) Separation and integration of the differential equation in x leads to a travel time based on the point of infiltration $t(x) = \frac{H\phi}{I} \ln \frac{L}{x}$. To get the steady-state travel time distribution, assume that the infiltration points are the random variable U uniformly distributed on $[0, L]$, so that the random time $T = \frac{H\phi}{I} \ln \frac{L}{U}$. The probability equality $P(U < x) = P(L \exp(\frac{-TI}{H\phi}) < x) = x/L$ leads to the distribution of travel time $P(T < t) = \exp(\frac{-tI}{H\phi})$. Similar to Paster et al. (2014), we can define dimensionless numbers for the transport characteristics of the aquifer as a whole and for the numerical method, which will have local mixing that depends on the number of particles. The mean residence time is $H\phi/I$, which leads us to define an aquifer-wide Peclet number $P_e = \frac{I}{H\phi}\frac{H^2}{D} = \frac{IH}{D\phi}$. In the case where mixing is given by a velocity-dependent dispersion, we use the approximation that the mean velocity is found at the mean distance $L/2$

(valid for small H), so that the mean dispersion time is $\frac{H^2}{\alpha LI/(2H\phi)}$, giving $P_e = \frac{2H^2}{\alpha L} = \frac{2H}{\alpha R}$, where R is the aquifer aspect ratio.

Supplementary material

Supplementary material associated with this article can be found, in the online version, at doi:10.1016/j.advwatres.2019.103386.

References

Benson, D.A., Aquino, T., Bolster, D., Engdahl, N., Henri, C.V., Fernàndez-Garcia, D., 2017. A comparison of Eulerian and Lagrangian transport and non-linear reaction algorithms. Adv. Water Resour. 99, 15–37. https://doi.org/10.1016/j.advwatres.2016.11.003.

Benson, D.A., Bolster, D., 2016. Arbitrarily complex chemical reactions on particles. Water Resour. Res. 52 (11), 9190–9200. https://doi.org/10.1002/2016WR019368.

Benson, D.A., Meerschaert, M.M., 2008. Simulation of chemical reaction via particle tracking: diffusion-limited versus thermodynamic rate-limited regimes. Water Resour. Res. 44, W12201. https://doi.org/10.1029/2008WR007111.

Benson, D.A., Pankavich, S., Bolster, D., 2019. On the separate treatment of mixing and spreading by the reactive-particle-tracking algorithm: an example of accurate upscaling of reactive poiseuille flow. Adv. Water Resour. 123, 40–53. https://doi.org/10.1016/j.advwatres.2018.11.001.

Benson, D.A., Pankavich, S., Schmidt, M., Sole-Mari, G., 2019. Entropy: the former trouble with particles (including a new numerical model computational penalty for the akaike information criterion). submitted.

Bolster, D., Paster, A., Benson, D.A., 2016. A particle number conserving Lagrangian method for mixing-driven reactive transport. Water Resour. Res. 52 (2), 1518–1527. https://doi.org/10.1002/2015WR018310.

Cirpka, O.A., Chiogna, G., Rolle, M., Bellin, A., 2015. Transverse mixing in three-dimensional nonstationary anisotropic heterogeneous porous media. Water Resour. Res. 51 (241–260). https://doi.org/10.1002/2014WR015331.

Cornaton, F., Perrochet, P., 2006. Groundwater age, life expectancy and transit time distributions in advective–dispersive systems: 1. Generalized reservoir theory. Adv. Water Resour. 29 (9), 1267–1291. https://doi.org/10.1016/j.advwatres.2005.10.009.

Cornaton, F.J., 2012. Transient water age distributions in environmental flow systems: the time-marching Laplace transform solution technique. Water Resour. Res. 48 (3), 1–17. https://doi.org/10.1029/2011WR010606.

Engdahl, N.B., Ginn, T.R., Fogg, G.E., 2012. Non-Fickian dispersion of groundwater age. Water Resour. Res. 48 (7). https://doi.org/10.1029/2012WR012251.

Engdahl, N.B., McCallum, J.L., Massoudieh, A., 2016. Transient age distributions in subsurface hydrologic systems. J. Hydrol. 543, 88–100. https://doi.org/10.1016/j.jhydrol.2016.04.066.

Engdahl, N.B., Schmidt, M.J., Benson, D.A., 2019. Accelerating and parallelizing Lagrangian simulations of mixing-limited reactive transport. Water Resour. Res. 55. https://doi.org/10.1029/2018WR024361.

Ginn, T.R., 1999. On the distribution of multicomponent mixtures over generalized exposure time in subsurface flow and reactive transport: foundations, and formulations for groundwater age, chemical heterogeneity, and biodegradation. Water Resour. Res. 35 (5), 1395–1407.

Goode, D.J., 1996. Direct simulation of groundwater age. Water Resour. Res. 32 (2), 289–296. https://doi.org/10.1029/95WR03401.

Green, C.T., Liao, L., Nolan, B.T., Juckem, P.F., Shope, C.L., Tesoriero, A.J., Jurgens, B.C., 2018. Regional variability of nitrate fluxes in the unsaturated zone and groundwater, Wisconsin, USA. Water Resour. Res. 54 (1), 301–322. https://doi.org/10.1002/2017WR022012.

Herrera, P.A., Valocchi, A.J., Beckie, R.D., 2010. A multidimensional streamline-based method to simulate reactive solute transport in heterogeneous porous media. Adv. Water Resour. 33 (7), 711–727. https://doi.org/10.1016/j.advwatres.2010.03.001.

Koh, E.-H., Lee, E., Kaown, D., Green, C.T., Koh, D.-C., Lee, K.-K., Lee, S.H., 2018. Comparison of groundwater age models for assessing nitrate loading, transport pathways, and management options in a complex aquifer system. Hydrological Process. 32 (7), 923–938. https://doi.org/10.1002/hyp.11465.

Labolle, E.M., Fogg, G.E., Tompson, A.F.B., 1996. Random-walk simulation of transport in heterogeneous porous media: local mass-conservation problem and implementation methods. Water Resour. Res. 32 (3), 583–593.

Massoudieh, A., Dentz, M., Alikhani, J., 2017. A spatial Markov model for the evolution of the joint distribution of groundwater age, arrival time, and velocity in heterogeneous media. Water Resour. Res. 53 (7), 5495–5515. https://doi.org/10.1002/2017WR020578.

Paster, A., Bolster, D., Benson, D.A., 2014. Connecting the dots: semi-analytical and random walk numerical solutions of the diffusion–reaction equation with stochastic initial conditions. J. Comput. Phys. 263, 91–112. https://doi.org/10.1016/j.jcp.2014.01.020.

Sanz-Prat, A., Lu, C., Finkel, M., Cirpka, O.A., 2015. On the validity of travel-time based nonlinear bioreactive transport models in steady-state flow. J. Contaminant Hydrol. 175, 26–43. https://doi.org/10.1016/j.jconhyd.2015.02.003.

Schmidt, M.J., Pankavich, S.D., Benson, D.A., 2018. On the accuracy of simulating mixing by random-walk particle-based mass-transfer algorithms. Adv. Water Resour. 117, 115–119. https://doi.org/10.1016/j.advwatres.2018.05.003.

Sole-Mari, G., Schmidt, M.J., Pankavich, S.D., Benson, D.A., 2019. Numerical equivalence between SPH and probabilistic mass transfer methods for Lagrangian simulation of dispersion. Adv. Water Resour. 126, 108–115. https://doi.org/10.1016/j.advwatres.2019.02.009.

Varni, M., Carrera, J., 1998. Simulation of groundwater age distributions. Water Resour. Res. 34 (12), 3271–3281.

Weissmann, G.S., Zhang, Y., LaBolle, E.M., Fogg, G.E., 2002. Dispersion of groundwater age in an alluvial aquifer system. Water Resour. Res. 38 (10), 16–1—16–13. https://doi.org/10.1029/2001WR000907.